Neutron diffraction at simultaneous high temperatures and pressures, with measurement of temperature by neutron radiography

Article *in* Mineralogical Magazine · December 2001

DOI: 10.1180/0026461016560005 · Source: OAI

15 authors, including:

Martin Travis Dove
Queen Mary, University of London
452 PUBLICATIONS **13,047** CITATIONS
SEE PROFILE

Simon Charles Kohn
University of Bristol
158 PUBLICATIONS **4,650** CITATIONS
SEE PROFILE

Geoffrey David Price
University College London
297 PUBLICATIONS **11,144** CITATIONS
SEE PROFILE

Simon Redfern
Nanyang Technological University
398 PUBLICATIONS **9,049** CITATIONS
SEE PROFILE

Mineralogical Magazine, December 2001, Vol. 65(6), pp. 737–748

Neutron diffraction at simultaneous high temperatures and pressures, with measurement of temperature by neutron radiography

Y. Le Godec[1], M. T. Dove[1,*], D. J. Francis[2], S. C. Kohn[3], W. G. Marshall[2], A. R. Pawley[4], G. D. Price[5], S. A. T. Redfern[1], N. Rhodes[2], N. L. Ross[5,†], P. F. Schofield[6], E. Schooneveld[2], G. Syfosse[7], M. G. Tucker[1] and M. D. Welch[6]

[1] Department of Earth Sciences, University of Cambridge, Downing Street, Cambridge CB2 3EQ, UK
[2] ISIS Facility, Rutherford Appleton Laboratory, Chilton, Didcot, Oxfordshire OX11 0QX, UK
[3] Department of Earth Sciences, University of Bristol, Wills Memorial Building, Queen's Road, Bristol BS8 1RJ, UK
[4] Department of Earth Sciences, University of Manchester, Oxford Road, Manchester M13 9PL, UK
[5] Department of Geological Sciences, University College London, Gower Street, London WC1E 6BT, UK
[6] Department of Mineralogy, Natural History Museum, Cromwell Road, London SW7 5BD, UK
[7] Physique des Milieux Condensés, Université Pierre et Marie Curie, 75252 Paris, France

ABSTRACT

The commissioning and operation of apparatus for neutron diffraction at simultaneous high temperatures and pressures is reported. The basic design is based on the Paris-Edinburgh cell using opposed anvils, with internal heating. Temperature is measured using neutron radiography. The apparatus has been shown in both on-line and off-line tests to operate to a pressure of 7 GPa and temperature of 1700°C. The apparatus has been used in a neutron diffraction study of the crystal structure of deuterated brucite, and results for 520°C and 5.15 GPa are presented. The diffraction data that can be obtained from the apparatus are of comparable quality to previous high-pressure studies at ambient temperatures, and are clearly good enough for Rietveld refinement analysis to give structural data of reasonable quality.

Keywords: neutron diffraction, high temperature, high pressure, neutron radiography, Rietveld refinement.

Introduction

The pioneering work of Jean-Michel Besson, Richard Nelmes and co-workers has enabled neutron diffraction from samples at high pressures using time-of-flight methods to become feasible for routine studies (Besson *et al.*, 1992; Nelmes *et al.*, 1993; Besson and Nelmes, 1995). The work of this group has led to the development of the Paris-Edinburgh (PE) cell, in which pressure is applied using two opposed anvils mounted in a way that permits use of sample volumes that are large enough for neutron beams. Examples of minerals studied using PE cells include brucite (Parise *et al.*, 1993; Catti *et al.*, 1995), portlandite (Pavese *et al.*, 1997), FeS (Marshall *et al.*, 2000), FeSi (Wood *et al.*, 1995, 1996), hydrogarnet (Lager and von Dreele, 1996, 1997), cristobalite (Dove *et al.*, 2000), muscovite (Catti *et al.*, 1994), gypsum (Stretton *et al.*, 1997) and Phase A (Kagi *et al.*, 2000), in addition to a variety of ice phases (Loveday *et al.*, 1997; Klotz *et al.*, 1999). Neutron diffraction is a particularly useful method for the *in situ* study of mineral crystal structures for several reasons, including the high sensitivity of neutrons to H atoms, the relatively high scattering power of oxygen atoms compared to heavier metallic ions,

Dedicated to the memory of Prof. Jean-Michel Besson (Paris, 1936–2001)

* E-mail: martin@esc.cam.ac.uk
† Present address: Department of Geological Sciences, Virginia Tech, 4044 Derring Hall, Blacksburg, VA 24061, USA

DOI: 10.1180/002646101656000 5

the ability to study magnetic structures, and the fact that the form factor for nuclear scattering is independent of scattering vector.

Until recently, the PE technology could only be used at ambient temperatures or lower. Zhao *et al.* (1999) reported the development of an internal heating version of the PE cell, and used this for a study of the equation of state of molybdenum (Zhao *et al.*, 2000). The ability to perform diffraction measurements at simultaneous high pressures and temperatures will allow us to perform *in situ* crystallographic studies of minerals under conditions approaching those of the inner earth. In this paper we report the independent development and commissioning of a PE cell with internal heating that differs in several respects from that of Zhao *et al.* (1999). The cell has now been tested up to simultaneous pressures and temperatures of 7 GPa and 1700°C respectively. We also report here the first results from the use of the internal-heating high-*P/T* PE cell in a study of deuterated brucite. Brucite was chosen for the test case because it has a crystal structure that is non-trivial whilst not being unnecessarily complicated, because there are ambient-temperature high-pressure results available for comparison (Parise *et al.*, 1993; Catti *et al.*, 1995), and because it is a hydrous phase.

The issue of measurement of temperature at high pressures is not trivial. In principle, thermocouples could be used, as in the apparatus of Zhao *et al.* (1999). However, a previous study on the effect of pressure on the emf induced in a standard Chromel-Alumel thermocouple has indicated that the corrections are important in high-pressure and high-temperature measurements (Getting and Kennedy, 1970). Furthermore, these corrections have been measured only to 3.3 GPa, and no reliable pressure correction exists for higher pressures. In addition to these general issues, insertion of a thermocouple into a typical PE set-up has several other disadvantages. These include: (1) The thermocouple will displace a considerable fraction of the gasket, which will reduce the mechanical performance. During our preliminary tests, we observed that this was the source of all blow-out failures at high pressure and temperature. (2) The thermocouple will introduce imperfections into the furnace by creating a hole, which will increase the possibility of furnace rupture, and give rise to thermal leaks of the set-up, which will lead to non-uniform thermal gradients inside the sample. (3) To record an accurate sample temperature, it is necessary to introduce the thermocouple through the sample capsule. This configuration may give rise to a diffraction signal from the thermocouple which will contaminate the diffraction pattern from the sample. There may also be occasions when thermocouple materials will react chemically with the sample, or when the sample needs to be loaded in a liquid state. (4) When the sample assembly is under pressure, the size of the gap between anvils will be of the same order as the outside diameter of the thermocouple. Thus it reduces the ability to reach higher pressures when heating. (5) Any thermocouple will become the critical part of the set-up. The experiments will depend on the success of the thermocouple, since breakage of the thermocouple will mean the end of the experimental run. Breakages are not infrequent, and we have found that thermocouples can only survive the application of pressure if the sample can be pressed into a pellet prior to loading into the high-*P/T* assembly.

We have therefore explored the possibility of using neutron absorption resonance radiography (NARR) methods to determine the temperature (Fowler and Taylor, 1987; Mayers *et al.*, 1989). This is a non-invasive method for measuring temperature, in contrast to the use of thermocouples. As discussed below, it is also relatively quick. The NARR approach has the disadvantage of requiring an explicit measurement, and does not provide any control or pre-setting capabilities. However, we show here that the radiography method is simple to implement, and gives precision to within ± 20 K.

The programme of work reported in this paper has been carried out on the high-pressure facility, HiPr, of the PEARL beamline at the ISIS spallation neutron source (UK). There are technical advantages in using a time-of-flight neutron source with energy-dispersive measurements for high-pressure studies as compared to a steady-state source with angle-dispersive measurements, not least because it is possible to use a small fixed range of scattering angles around 90° to facilitate effective beam collimation and reduction of scattering from the sample environment.

Paris-Edinburgh cell with internal heating

The basic design of our PE cell with internal heating is shown in Fig. 1. The principle of the PE cell is that the sample is confined within a gasket, which is held between two opposed anvils. For

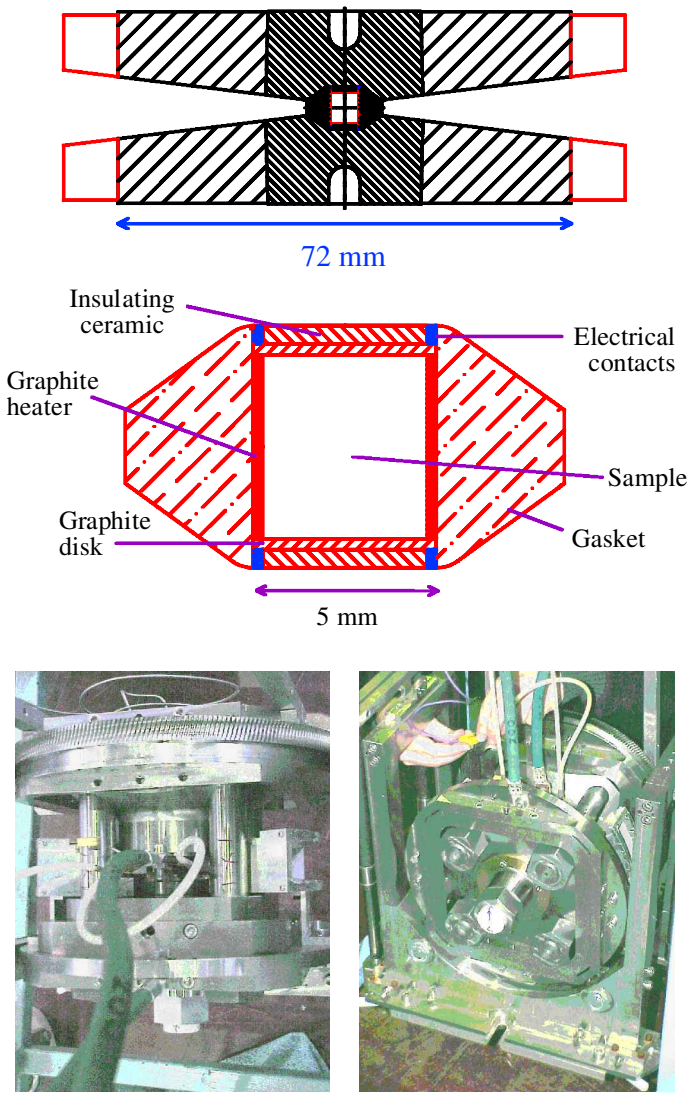

FIG. 1. (Upper) Schematic design of the anvil assembly of the Paris-Edinburgh cell. (Middle) Schematic design of internal heating components. (Lower) Photographs of the Paris-Edinburgh cell with power supplies connected.

our work, we have substantially modified the geometry of the anvils compared to their usual design. To date, all neutron diffraction experiments using the PE cell use a toroidal shape for the anvils (Besson and Nelmes, 1995). In order to maximize the volume of the sample, we developed a new geometry for the WC anvils with a conical profile. This is preferable to the hemispherical shape because of its mechanical strength, compression efficiency, and reduction in uniaxial stress (Le Godec, 1999).

The sample, which is usually mixed with an internal calibrant powder such as NaCl or MgO, is located inside a high-resistivity graphite furnace. This serves both as a heater and as a pressure transmitter. The heat is generated by an electrical current, which reaches the graphite heater through the anvils and the electrical contacts. The

assembly of sample and furnace is then loaded into a ceramic gasket. The choice of the gasket material is crucial. We tested many gasket materials, including magnesium oxide, zirconium phosphate (as used by Zhao *et al.*, 1999), zircon and pyrophyllite, against the following criteria: (1) the gasket must be a good electric and thermal insulator; (2) the gasket must have sufficient mechanical strength to support high pressures at high temperatures; (3) the gasket must not have a significant plastic flow within our new anvil geometry and high pressures and temperatures; and (4) the gasket must have low absorption and minimum scattering of the neutron beams.

We eventually selected pyrophyllite for the gasket material, having demonstrated its excellent thermal and mechanical properties in tests performed at the French synchrotron LURE and at the European Synchrotron Radiation Facilities ESRF. Tests of its neutron transparency after thermal treatment were carried out at ISIS. These tests will be described in more detail elsewhere (Le Godec *et al.*, in press.). We also found that a confining ring of Teflon placed around the gasket is necessary to maintain the integrity of the pyrophyllite gasket at high pressures and temperatures. The geometry of this ring has been optimized to improve the efficiency of the compression and, hence, to give the maximal pressure.

Another important criterion is that the equipment should have excellent stability of pressure and temperature over the time scales of a neutron diffraction measurement. The time scale for a measurement is significantly longer than for a synchrotron X-ray diffraction experiment, which is typically <1 h. Temperature stability is achieved using a regulated power supply. For example, in off-line tests, a sample held under pressure at 1000°C showed a maximum drift of the temperature of less than ± 2°C for over 8 h.

The major source of pressure instability during high *P/T* experiments comes from an increase in the temperature of the anvils. Specifically, at high pressures and temperatures, the hot anvils increase the temperature of the oil in the PE cell, leading to an increase in the oil pressure and hence an increase in the pressure in the sample. In order to solve this problem, we developed a cooling system involving water circulation around the anvils. We found that this device is very effective, and gives the required pressure stability. Further details will be published elsewhere (Le Godec *et al.*, in press.).

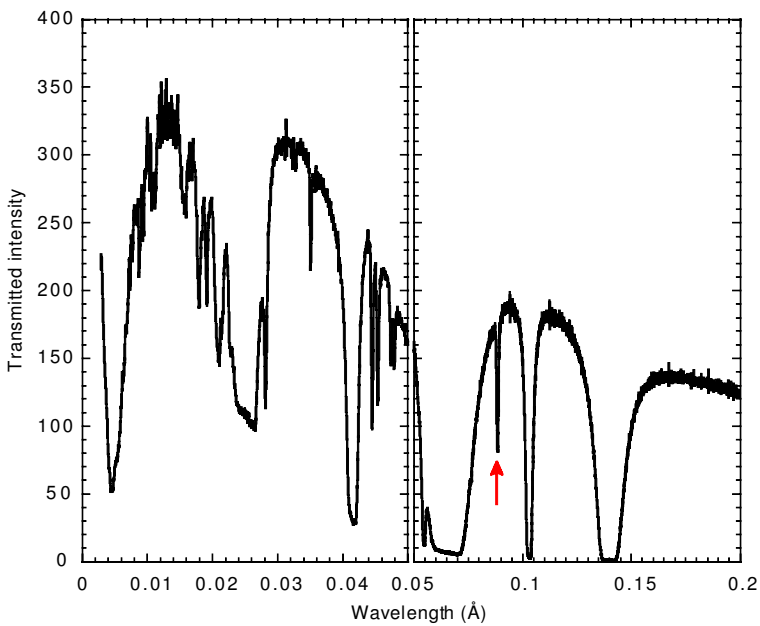

FIG. 2. Neutron absorption spectrum of the high-pressure/temperature Paris-Edinburgh cell containing a foil of tantalum. The resonance line from the tantalum foil used in the present analysis is marked by an arrow.

To summarize, we have shown that our equipment is able to generate stable pressures to 7 GPa, and stable temperatures to 1700°C, on a set-up with a sample volume of 65 mm^3. The performance can be increased further with reduction in sample volume.

Measurement of temperature using neutron absorption resonance radiography

Basic idea

The idea of using NARR as a means of determining sample temperature was initially pioneered by Fowler and Taylor (1987), and developed further by Mayers and co-workers (Mayers *et al.*, 1989; Frost *et al.*, 1989). The basic idea is to measure the energy or wavelength dependence of the neutron absorption resonance by a heavy atom in a heated sample. The width of the resonance will be increased by the Doppler effect from the thermal motions of the atoms in the sample. If a simple metal is used, the phonon frequencies will be relatively low, and for temperatures above the Debye temperature the vibrational amplitudes will be given by classical equipartition and will be independent of the force constants. As a result, the width of the resonance should be independent of pressure.

Fowler and Taylor (1987) provided information about a number of potential atomic nuclei that can be used for NARR measurements. We use tantalum as our absorbing foil. This choice was partly determined by the resonance spectrum of the empty PE cell. The various pieces of the high-pressure equipment contain many metals as primary or trace components (e.g. tungsten, nickel), as shown in Fig. 2. A useful resonance is at 10.34 eV, with corresponding wavelength 8.9 pm. Fowler and Taylor (1987) noted the Doppler effect of this resonance should be relatively easy to measure, and it is well separated from other resonances in the absorption spectrum. For this work, we used a foil disk of 50 μm.

Radiography detector

For our NARR experiments a new high-efficiency neutron monitor for HiPr was developed. This is based on a scintillation detector. The active scintillation element is a ^{6}Li-enriched glass, with dimensions 7×7 mm in cross-section and 25 mm deep in the direction of the neutron beam. One of the long faces is viewed by a ten-stage linear photomultiplier tube. The photomultiplier tube and scintillation block is surrounded by a thin (50 μm) cylindrical aluminium foil reflector to enhance light collection. The components are shown in Fig. 3. The detector exhibits good pulse height resolution, and to a first approximation, the neutron detector efficiency is close to the neutron absorption efficiency, which was calculated to be 75% at 10 eV.

Analysis of resonance spectra

The exact expression for the width of the resonance line depends on a number of factors, some of which are geometric in origin. In the earlier work of Fowler and Taylor (1987) and Mayers *et al.* (1989), a first-principles analytical analysis was discarded in favour of an empirical analysis, by comparing measurements against calibrations. These workers considered the ratio of the absorption spectrum at a given temperature with that at ambient temperature; the ratio spectra obtained from our measurements are shown in Fig. 4. The shapes of these ratio spectra are not symmetric about the midpoint, which is primarily due to the sloping backgrounds. Therefore we chose instead to use curve fitting on the raw spectra, and extract the fitted widths of the resonance lines as the fundamental quantity. We found, somewhat surprisingly, that the absorption profiles could be fitted accurately using Gaussian functions:

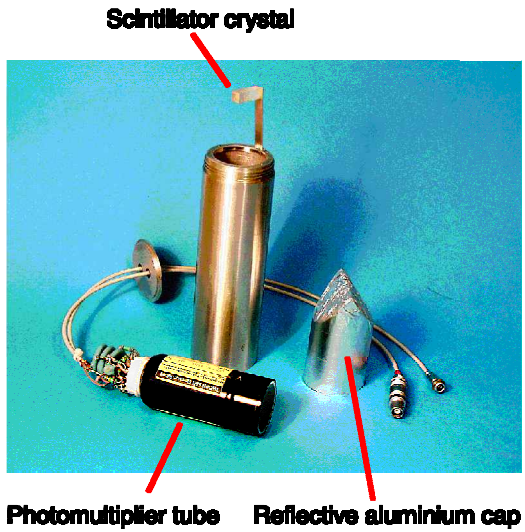

FIG. 3. Components of the neutron resonance monitor.

$$I = I_0 \exp(-(\lambda - \lambda_0)^2/2\sigma^2)$$

where λ_0 is the midpoint of the resonance when plotted as beam wavelength, λ, I_0 is the peak absorbance, and σ is the width of the peak resonance. Examples of two fitted absorption profiles are shown in Fig. 5.

The approach we have chosen to work with is to carry out a series of calibration runs with a thermocouple and a small ceramic pellet, with the sample assembly under nominally zero pressure – actually a small load is applied to the cell in order to lock the components in place. Measurements of the resonance spectrum were performed for temperatures to 1000°C. The squares of the fitted widths, σ^2, of one set of calibration curves are shown as a function of temperature in Fig. 6. The data can be fitted by a straight line. Different series of calibration tests showed that the slope of this line is a constant, independent of the actual experimental configuration. However, we find small offsets of the line for different sample loadings. This offset can be easily calibrated in a measurement at ambient temperature for any new sample loading. A number of tests have shown that the resonance line width at ambient temperature is independent of pressure, as anticipated in our description of the basic principles above. The first data, which are reported here, are of lower accuracy than our more recent tests, which show an accuracy to within ±20 K. We have identified strategies to improve the accuracy further, and these will be discussed elsewhere. It should be noted that the typical accuracy of thermocouples is of the order of ±1%, which is equivalent to an accuracy of ±10 K at 1000 K, and our calibration has relied on thermocouple measurements.

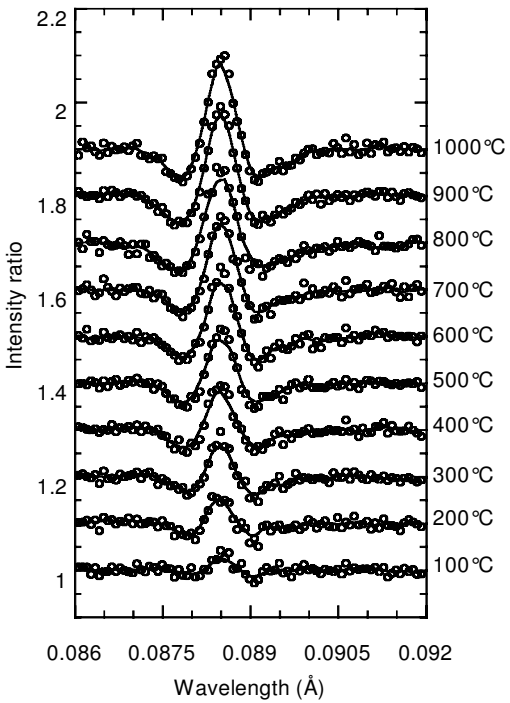

FIG. 4. Ratios of the tantalum resonance spectra at various temperatures with that at ambient temperature.

Commissioning experiment: deuterated brucite at high pressures and temperatures

Experimental details

The high-*P/T* apparatus was used for a crystallographic study of deuterated brucite. The sample was prepared following the method of Parise *et al.* (1993). The sample of brucite was mixed with powdered NaCl in a ratio of 3:2. The NaCl had two roles, first to assist with pressure transmission through the sample, and the second to give a calibration of the pressure following the measurement of the equation of state (Decker, 1971).

Measurements of the diffraction pattern were obtained on the PEARL beamline at ISIS for various pressures and temperatures following sequences in which either sample loading or temperature were changed separately. Eventually the sample was heated above 800°C at 5.2 GPa, at which point the brucite decomposed. This decomposition reaction is catalysed by the reaction of brucite with the NaCl used for calibration and pressure transmission (Shmulovich and Graham, 1996).

Results

The diffraction pattern from a measurement at 5.15 GPa and 520°C is shown in Fig. 7. The crystal structure at each temperature was refined with the Rietveld method, using the GSAS program. Thermal motions of the atoms were represented using isotropic atomic displacement parameters. Two different structure models were used for all temperatures and pressures, one using a single position for the H atoms, and the other using a split-site representation for the positions of the H atoms. It should be noted that the splitting of the H over three sites may not imply

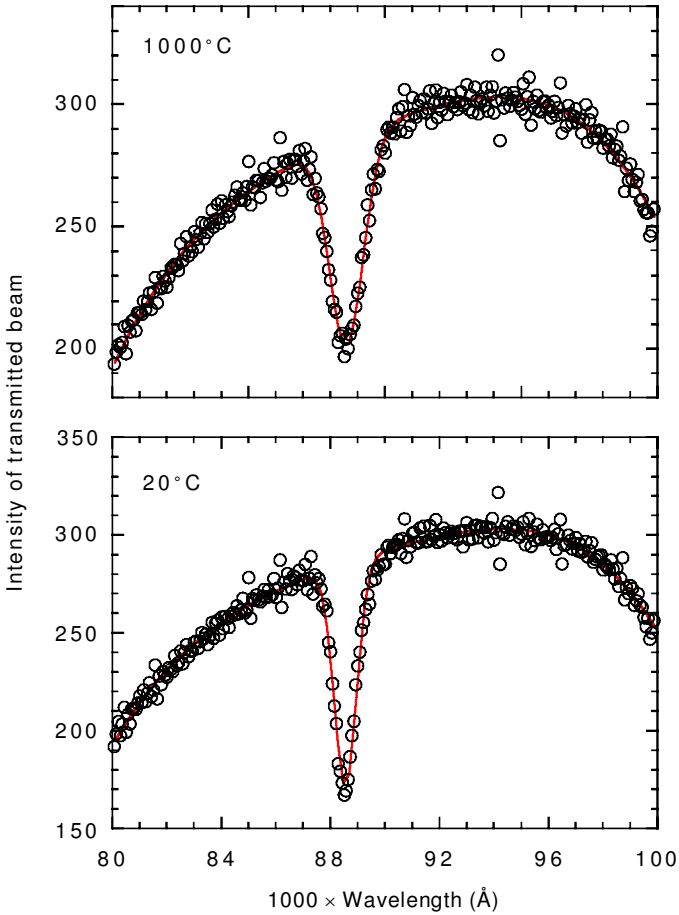

FIG. 5. Absorption resonance spectra of tantalum at 20°C and 1000°C fitted by a Gaussian function (red curve).

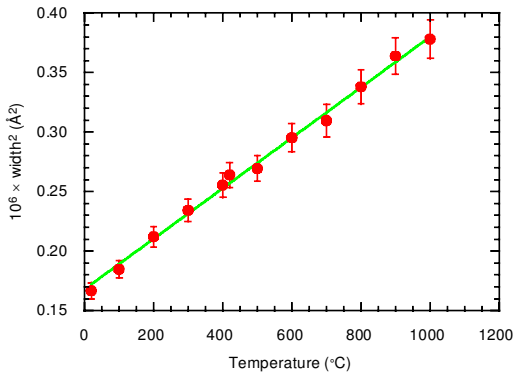

FIG. 6. Plot of the square of the tantalum absorption resonance line against temperature, fitted with a straight line.

static symmetry breaking, but provides a representation of a single site with highly anisotropic and anharmonic thermal motion. The details of the refined structure at 5.15 GPa and 520°C are presented in Table 1, and the structure shown in Fig. 8.

The key concern is the quality of the data that can be achieved with the high-*P/T* apparatus as compared with high-pressure measurements at ambient temperature, and here we compare measurements of the pressure-dependence of the unit-cell volume and O—D bond length with previously published data. In Fig. 9 we show the pressure-dependence of the volume of the unit cell at ambient temperature. The data are compared with the data for $Mg(OD)_2$ of Parise *et al.* (1993) and the data for $Mg(OH)_2$ of Catti *et*

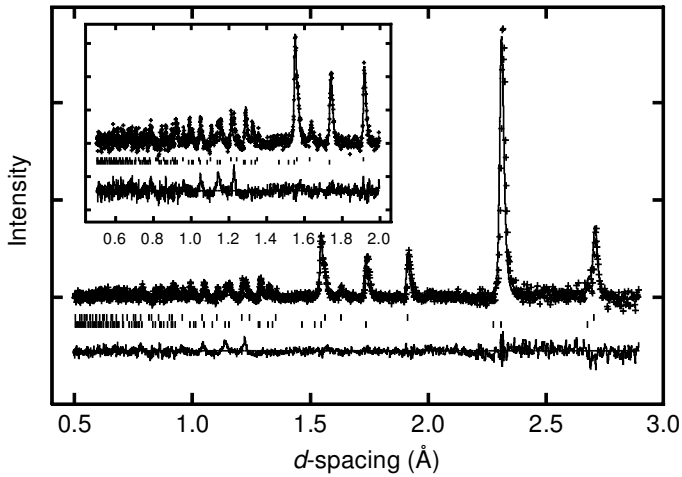

FIG. 7. Diffraction pattern of deuterated brucite at 5.4 GPa and 550°C. The curve is the result of a Rietveld refinement.

al. (1995). The latter data were also obtained at ISIS (on the Polaris diffractometer), and the former data were obtained at the IPNS source. The agreement between our data and the earlier data is very good. In Fig. 10 we show the pressure dependence of the O—D bond length at ambient temperature. The bond length is extracted from the results of the Rietveld structure refinements, and in Fig. 10 we show the results from both the single-site and split-site models for the H atoms. The single-site O—D distance is slightly shorter than that from the split-site model, which is consistent with our interpretation of this model in terms of thermal motion. The split-site O—D distances compare well with the distances from Parise *et al.* (1993). Catti *et al.* (1995) used only a single-site model for the H positions, but corrected their O—H distances for thermal motions. This leads to a lowering of the O—H distances, consistent with our data. Both the uncorrected and corrected distances of Catti *et al.* (1995) are shown in Fig. 10.

TABLE 1. Structural parameters for $Mg(OD)_2$ at 5.15 GPa and 520°C obtained from Rietveld refinement using both single-site and three-site representations of the positions of the D atoms (as described in the text). The space group is $P\bar{3}m1$. Mg fractional coordinates are 0,0,0; O fractional coordinates are 1/3,2/3,*z*; D coordinates in the single-site model are 1/3,2/3,*z*; and D fractional coordinates in the three-site model are *x*,2*x*,*z*. Values for the thermal displacement parameters are not reported because they are affected by beam absorption.

	Single site	Three-site
a (Å)	3.0987(3)	3.0987(3)
c (Å)	4.5631 (12)	4.5628 (12)
Unit cell volume (Å^3)	37.945 (8)	37.943 (8)
O(*z*)	0.217 (4)	0.220 (3)
D(*z*)	0.393 (7)	0.405 (5)
D(*x*)	—	0.271 (5)
O—D length (Å)	0.81 (2)	0.91 (2)

Results for the volume of the unit cell for the sample temperatures and pressures used in the experiment are shown in Fig. 11. Increasing temperature can cause a slight change in pressure, and changing pressure can lead to a small change in temperature for constant power, so we are not able to report systematic measurements. However, the effects of increasing both temperature and pressure, leading to expansion and contraction respectively, are clear from Fig. 11. From the Rietveld refinements we also obtained the O—D distance as a function of both temperature and pressure. Within the error bars, this distance appears to have little dependence on either temperature or pressure. A more detailed analysis of the crystallographic data will be presented elsewhere.

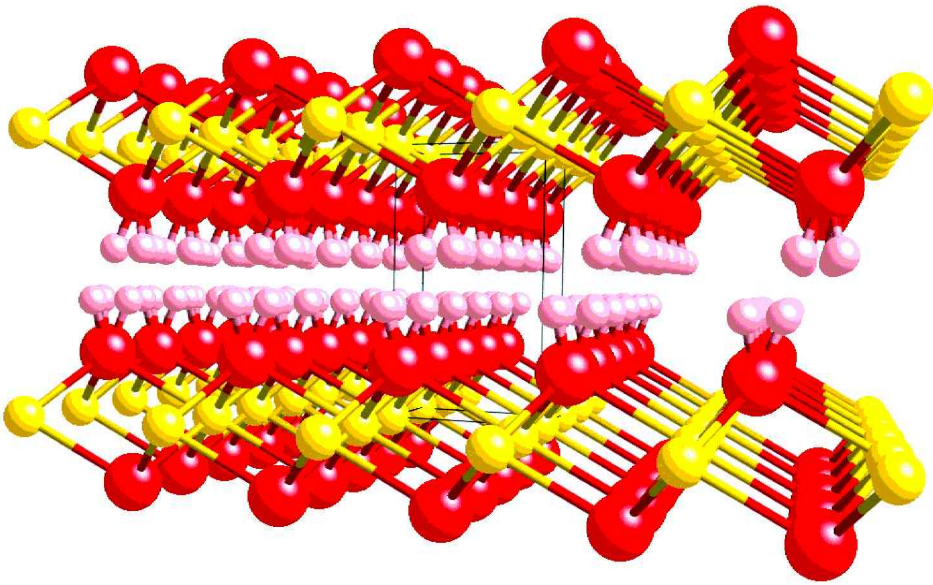

FIG. 8. Crystal structure of deuterated brucite refined from the diffraction data at 5.4 GPa and 550°C, showing the split sites for the H atoms.

Finally, we also report an important observation, which is summarized in Fig. 12. It is often found that increasing pressure leads to a broadening of Bragg peaks due to pressure gradients established in the sample. We found the same for our samples. However, on heating, the Bragg peaks are sharpened back to their initial widths. In

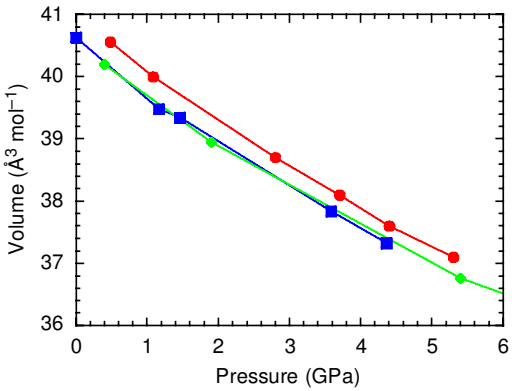

FIG. 9. Pressure dependence of the volume of the unit cell at ambient temperature obtained in the present experiments (blue squares and connecting lines), compared with the data from Parise *et al.* (1993) on a deuterated sample (green diamonds and connecting lines), and from Catti *et al.* (1995) on a hydrogenated sample (red circles and connecting lines).

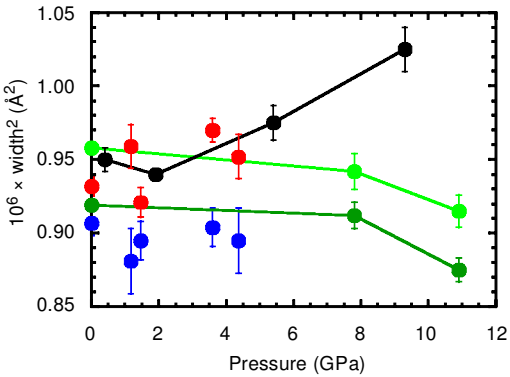

FIG. 10. Pressure dependence of the O–H bond length obtained at ambient temperature in the present study, showing the distances for both single-site (blue) and split-site (red) refinements of the hydrogen positions, which are compared with the results from the split-site refinements of Parise *et al.* (1993) (black, with connecting lines) and the results from the single-site refinements of Catti *et al.* (1995) with (light green, with connecting lines) and without (dark green, with connecting lines) corrections for thermal motion.

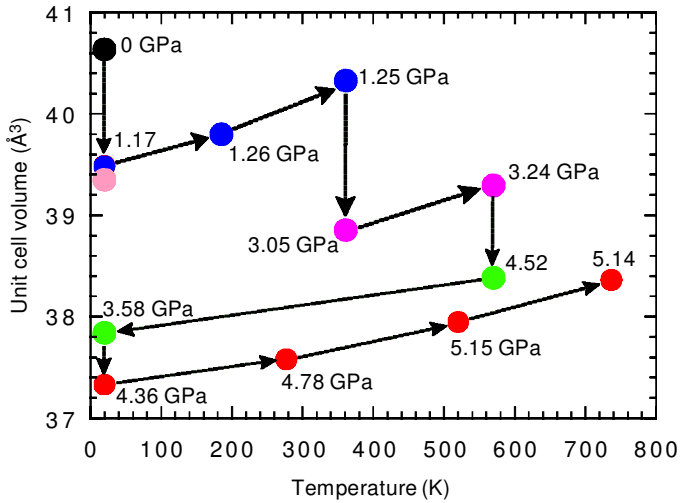

FIG. 11. Temperature and pressure dependence of the volume of the unit cell. The numbers associated with each point give the pressure of the measurement (GPa). Different loadings are shown with different colours, and the lines with arrows indicate the sequence of changing pressure and/or temperature.

Fig. 12 we show a compression/heating cycle. At each point in the cycle, the width of the Bragg peak obtained from the Rietveld refinement is noted. The important point is that at ambient temperature, the width of the Bragg peaks increased on increasing pressure, but on heating, the widths reduced to their initial values, and we found that they remain sharp after cooling to ambient temperature. The sharpening of the Bragg peaks arises because annealing at elevated temperature enables the deviatoric stresses to be relieved spontaneously, and this annealing is effective even after cooling back to ambient temperature. This suggests that internal heating

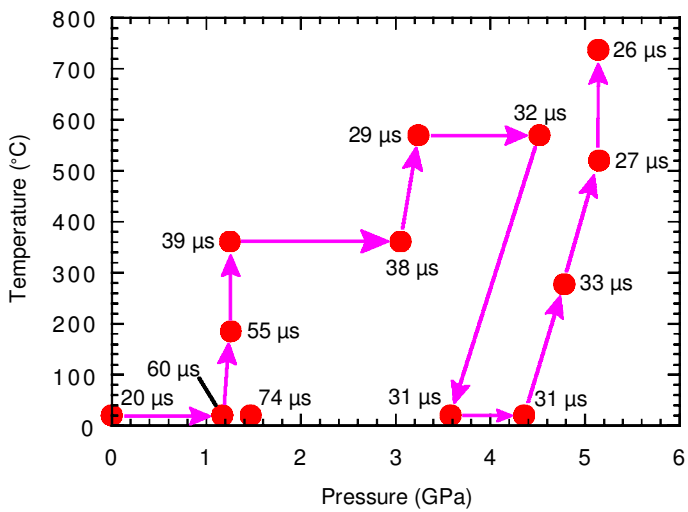

FIG. 12. Schematic plot of the effect of temperature on the widths of the Bragg diffraction peaks. The points and lines with arrows indicate the cycle of measurements, and the numbers give the refined values of the Gaussian line widths.

may be useful simply as a means of reducing pressure gradients, even if temperature is not of direct interest in the experiment.

Conclusion

We have reported the development and testing of a version of the Paris-Edinburgh cell for high-pressure time-of-flight neutron diffraction studies with internal heating. The cell has been tested to 7 GPa and 1700°C, and work is being carried out to extend these limits. One of the novel features of our apparatus is the use of neutron absorption resonance radiographic methods for measurement of temperature.

Acknowledgements

The work has been funded by NERC. We are grateful for support from Richard Nelmes and John Loveday (Edinburgh/ISIS), and from Stefan Klotz and Gerard Hamel (Paris). Above all, we acknowledge the essential inspiration, help and guidance given by the late Jean-Michel Besson, to whom we have dedicated this paper.

References

Besson, J.M. and Nelmes, R.J. (1995) New developments in neutron-scattering methods under high pressure with the Paris-Edinburgh cells, *Physica B*, **213**, 31–6.

Besson, J.M., Nelmes, R.J., Hamel, G., Loveday, J.S., Weill, G. and Hull, S. (1992) Neutron powder diffraction above 10 GPa. *Physica B*, **180**, 907–10.

Catti, M., Ferraris, G., Hull, S. and Pavese, A. (1994) Powder neutron-diffraction study of 2M1 muscovite at room pressure and at 2 GPa. *Eur. J. Mineral.*, **6**, 171–8.

Catti, M., Ferraris, G., Hull, S. and Pavese, A. (1995) Static compression and H-disorder in brucite, $Mg(OH)_2$, to 11 GPa – a powder neutron-diffraction study. *Phys. Chem. Miner.*, **22**, 200–6.

Decker, D.L. (1971) High-pressure equation of state for NaCl, KCl and CsCl, *J. Appl. Phys.*, **42**, 3239–44.

Dove, M.T., Craig, M.S., Keen, D.A., Marshall, W.G., Redfern, S.A.T., Trachenko, K.O. and Tucker, M.G. (2000) Crystal structure of the high-pressure monoclinic phase-II of cristobalite, SiO_2. *Mineral. Mag.*, **64**, 569–76.

Fowler, P.H. and Taylor, A.D. (1987) *Temperature imaging using epithermal neutrons*. Rutherford Appleton Laboratory Report RAL-87-056.

Frost, J.C., Meehan, P., Morris, S.R., Ward, R.C. and Mayers, J. (1989) Non-intrusive temperature-measurement of the components of a working catalyst by neutron resonance radiography. *Catalysis Letters*, **2**, 97–104.

Getting, I.C. and Kennedy, G.C. (1970) Effect of pressure on the emf of chromel-alumel and platinum-platinum 10% rhodium thermocouples, *J. Appl. Phys.*, **41**, 4552–62.

Kagi, H., Parise, J.B., Cho, H., Rossman, G.R. and Loveday, J.S. (2000) Hydrogen bonding interactions in phase A $\{Mg_7Si_2O_8(OH)_6\}$ at ambient and high pressure. *Phys. Chem. Miner.*, **27**, 225–33.

Klotz, S., Besson, J.M., Hamel, G., Nelmes, R.J., Loveday, J.S. and. Marshall, W.G. (1999) Metastable ice VII at low temperature and ambient pressure. *Nature*, **398**, 681–4.

Lager, G.A. and Von Dreele, R.B. (1996) Neutron powder diffraction study of hydrogarnet to 9.0 GPa. *Amer. Mineral.*, **81**, 1097–104.

Lager, G.A. and Von Dreele, R.B. (1997) Neutron powder diffraction study of hydrogarnet to 9.0 GPa (vol. 81, p. 1097, 1996). *Amer. Mineral.*, **82**, 212.

Le Godec, Y. (1999) *Étude du nitrure de bore sous hautes pression et temperature*. PhD Thesis, Univ. Denis Diderot, Paris VII.

Le Godec, Y., Dove, M.T., Redfern, S.A.T., Marshall, W.G., Tucker, M.G., Syfosse, G. and Besson, J.M. (2002) A new high P-T cell for neutron diffraction up to 7 GPa and 2000 K with measurement of temperature by neutron radiography. *High Press. Res.* (in press).

Loveday, J.S., Nelmes, R.J., Marshall, W.G., Besson, J.M., Klotz, S. and Hamel, G. (1997) Structural studies of ices at high pressure. *Physica B*, **241**, 240–6.

Marshall, W.G., Nelmes, R.J., Loveday, J.S., Klotz, S., Besson, J.M., Hamel, G. and Parise, J.B. (2000) High-pressure neutron diffraction study of FeS. *Phys. Rev. B*, **61**, 11201–4.

Mayers, J., Baciocco, G. and Hannon, A.C. (1989) Temperature-measurement by neutron resonance radiography. *Nuclear Instruments & Methods in Physics Research A*, **275**, 453–9.

Nelmes, R.J., Loveday, J.S., Wilson, R.M., Besson, J.M., Klotz, S., Hamel, G. and Hull, S. (1993) Structure studies at high pressure using neutron powder diffraction. *Trans. Amer. Crystallogr. Assoc.*, **29**, 19–27.

Parise, J.B., Leinenweber, K., Weidner, D.J., Tan, K. and von Dreele, R.B. (1993) Pressure-induced H-bonding – neutron-diffraction study of brucite, $Mg(OD)_2$, to 9.3 GPa. *Amer. Mineral.*, **79**, 193–6.

Pavese, A., Catti, M., Ferraris, G. and Hull, S. (1997) P-V equation of state of portlandite, $Ca(OH)_2$, from powder neutron diffraction data. *Phys. Chem. Miner.*, **24**, 85–9.

Shmulovich, K.I. and Graham, C.M. (1996) Melting of albite and dehydration of brucite in H_2O–NaCl fluids to 9 kbars and 700-900°C: implications for partial melting and water activities during high pressure metamorphism. *Contrib. Mineral. Petrol.*, **124**, 370–82.

Stretton, I.C., Schofield, P.F., Hull, S. and Knight, K.S. (1997) The static compressibility of gypsum. *Geophys. Res. Lett.*, **24**, 1267–70.

Wood, I.G., Chaplin, T.D., David, W.I.F., Hull, S., Price, G.D. and Street, J.N. (1995) Compressibility of FeSi between 0 and 9 GPa, determined by high-pressure time-of-flight neutron powder diffraction. *J. Phys: Cond. Matt.*, **7**, L475–9.

Wood, I.G., David, W.I.F., Hull, S. and Price, G.D. (1996) A high-pressure study of ε-FeSi, between 0 and 8.5 GPa, by time-of-flight neutron powder diffraction. *J. Appl. Crystallogr.*, **29**, 215–8.

Zhao, Y.S., von Dreele, R.B. and Morgan, J.G. (1999) A high P-T cell assembly for neutron diffraction up to 10 GPa and 1500 K. *High Press. Res.*, **16**, 161–77.

Zhao, Y.S., Lawson, A.C., Zhang, J.Z., Bennett, B.I. and Von Dreele, R.B. (2000) Thermoelastic equation of state of molybdenum. *Phys. Rev. B*, **62**, 8766–76.

{*Manuscript received 10 July 2001: revised 7 September 2001*}